Journal of Sound and Vibration 329 (2010) 2843–2850

Contents lists available at ScienceDirect

Journal of Sound and Vibration

journal homepage: www.elsevier.com/locate/jsvi

T-matrix method formulation applied to the study of flexural waves scattering from a through obstacle in a plate

V.V. Matus [a], V.F. Emets [b,*]

[a] *Pidstryhach Institute for Applied Problems of Mechanics and Mathematics, NASU 3 "B" Naukova St., 79601 Lviv, Ukraine*
[b] *Institute of Computer Science of Technical University of Lodz, Wolczanska 215, 93-005 Lodz, Poland*

ARTICLE INFO

Article history:
Received 17 March 2009
Received in revised form
20 November 2009
Accepted 4 January 2010
Handling Editor: A.V. Metrikine
Available online 24 February 2010

ABSTRACT

Elastic wave scattering in a flat thin plate hosting a through obstacle of arbitrary closed form is examined using a numerical technique based on the *T*-matrix approach, which is applied to describe of flexural waves in plates. The limiting cases of a hole and a rigid obstacle are considered. The vibrations of the plate are described by the Kirchhoff model. The far field backscattered amplitude as a function of wave frequency for inclusions of elliptic, triangular and square form with rounded corners is analysed numerically. Comparison of present results for circular obstacles with the analytical solutions obtained by other authors show excellent agreement.

1. Introduction

The guided waves in a low frequency-thickness product region can be successfully used to non-destructive evaluation of the large plate-like structures [1]. However, there are several complications which cause difficulties in the interpretation of the scattered fields when a propagating Lamb mode interacts with inhomogeneity of arbitrary closed geometry.

Scattering of elastic waves can occur if there exists incontinuity such as inclusion, crack and cavity in an elastic medium (see [2,3], for example). The analysis of elastic waves diffraction in thin plates with inhomogeneities of a cylindrical form is the subject, among others, of papers [4–18]. With the wave function expansion method, Pao and Chao [4] were the first who studied the problem of the flexural wave scattering and dynamic stress concentrations in Mindlin's plates with a circular hole and gave an analytical solution and numerical examples. Similar results were presented in [5] for a rigid inclusion. The theory of flexural waves scattering from an elastic heterogeneity of a circular shape in a flat thin plate is developed in papers [6–9]. McKeon and Hinders [10] have studied the interaction of the lowest order symmetric Lamb waves with a circular hole in a plate using Kane–Mindlin higher order plate theory and analytical expressions for the scattering waves are derived. Fromme and Sayir [11] presented modelling of flexural wave scattering by a through hole using Kirchhoff and Mindlin theory and near field measurements. Paskaramoorthy et al. [12] have used a finite element method (FEM) in combination with a wave function expansion technique to study the scattering of flexural waves by arbitrary shaped cavities in Mindlin's plates. Diligent et al. have presented FEM and experimental results for scattering of first symmetric Lamb mode from through holes [13] and flat bottomed holes [14]. Peng [15] presented the acoustical wave propagator technique to describe the flexural wave propagation and scattering in an elastic plate with multiple cylindrical patches using Kirchhoff's plate theory. The patches are made of the same material as the plate and the radius of the patches is comparable with the plate thickness. Wang and Chang [16] presented the scattering models based on a wave function expansion technique as well as the Born approximation for in-plane

* Corresponding author. Tel.: +48 42 631 27 97; fax: +48 42 630 34 14.
E-mail addresses: matus@iapmm.lviv.ua (V.V. Matus), wfemets@ics.p.lodz.pl (V.F. Emets).

0022-460X/$ - see front matter © 2010 Elsevier Ltd. All rights reserved.
doi:10.1016/j.jsv.2010.01.004

and flexural modes using the approximate plate wave theories. Grahn [17] investigated scattering of an incident plane symmetric Lamb wave mode from a circular partly through-thickness hole in a plate using both 3D theory and lowest order plate theories. The method which has been used is based on the mode expansions of the wave fields both in the inner region, below the hole, and in the outer region, outside the hole. A model and far field measurements for guided wave scattering from non-symmetric blind holes in isotropic plates using Poisson's and Mindlin plate wave theories for in-plane and flexural wave modes, respectively, was given by Cegla et al. [18].

The above publications have focused on the case of elastic wave scattering by circular inhomogeneities in a plate and there are little or no reported researches for the scattering of flexural wave by heterogeneity of a non-canonical form. For future applications of the guided waves in non destructive testing it would be very useful to use theoretical investigation of scattering flexural wave by a non-circular scatterer. Therefore, the purpose of the present paper is to consider scattering of flexural wave by a non-circular scatterer in a flat thin plate in the context of the Kirchhoff theory. Kirchhoff approximate theory is a widely used for describing motion in thin plates when the wavelength is much larger than the plate thickness and thus is only valid for low frequencies. Mindlin plate theory or 3D elasto-dynamic equations must be introduced in order to extend the range of frequencies [17,18].

An effective technique for analyzing the scattered field from an object of arbitrary closed form was proposed by Waterman [19]. This approach is well known as the *T*-matrix or null-field method. The *T*-matrix method has been used successfully to describe acoustic, electromagnetic and bulk elastic wave scattering by objects of complex geometry (see review paper [20], for example). In this article the *T*-matrix method is extended to describe the far field amplitude of flexural waves scattered from a non-circular region of inhomogeneity in the plate. The numerical results show the efficacy of the proposed method at low frequencies.

2. Problem statement and boundary integral relations

The elastic plate has thickness h, density ρ, Young's modulus E, and Poisson's ratio v. Scattering of an incoming plane flexural wave by a rigid or a soft through inclusion, contour of which is other than circular, is considered. All motions have frequency ω and time dependence $\exp(-i\omega t)$. The wave number is defined as $k=\sqrt[4]{\rho h\omega^2/D}$, where $D=Eh^3/12(1-v^2)$ is the flexural rigidity. Then equation of motion for the plate is

$$\Delta^2 w(\mathbf{r})-k^4 w(\mathbf{r})=0, \tag{1}$$

where Δ is the 2-D Laplacian, $w(\mathbf{r})=w^{in}(\mathbf{r})+w^{sc}(\mathbf{r})$ is a complete deflection of the median surface of the plate, $w^{in}(\mathbf{r})=A_0\exp(ik\mathbf{r}\cdot\mathbf{l})$ is the incoming field, $w^{sc}(\mathbf{r})$ is the reflected field, $\mathbf{r}=(x,y)$ is the radius-vector of the point of the median surface of the plate, (x,y) are the Cartesian co-ordinates with origin inside the heterogeneity, $\mathbf{l}=(\cos\theta_i,\sin\theta_i)$ is the direction of the wave incident. For a given direction $\mathbf{n}=(n_1,n_2)$ the bending moment M, generalized Kirchhoff stress V and normal slope γ at the point (r,θ) $(x=r\cos\theta,\ y=r\sin\theta)$ are

$$M=n_1^2M_r+2n_1n_2M_{r\theta}+n_2^2M_\theta, V=Q-\left(-n_2\frac{\partial}{\partial r}+n_1\frac{1}{r}\frac{\partial}{\partial\theta}\right)M_\tau, Q=-D\Delta\gamma(r,\theta).$$

$$M_\tau=(n_2^2-n_1^2)M_{r\theta}+n_1n_2(M_r-M_\theta),\quad M_r=-D\left[v\Delta+(1-v)\frac{\partial^2}{\partial r^2}\right]w(r,\theta),$$

$$M_\theta=-D\left[\Delta-(1-v)\frac{\partial^2}{\partial r^2}\right]w(r,\theta),\quad M_{r\theta}=-D(1-v)\frac{\partial}{r\,\partial\theta}\left(-\frac{1}{r}+\frac{\partial}{\partial r}\right)w(r,\theta),$$

$$\gamma=\left(n_1\frac{\partial}{\partial r}+n_2\frac{1}{r}\frac{\partial}{\partial\theta}\right)w(r,\theta). \tag{2}$$

The field $w^{sc}(\mathbf{r})$ satisfies the Sommerfeld radiation condition at infinity, from which it follows that:

$$w^{sc}(r,\theta)=A_0\sqrt{\frac{2}{\pi kr}}e^{i(kr-\pi/4)}f(\theta,\theta_i)+o(1/\sqrt{r}),\quad r\to\infty, \tag{3}$$

where $f(\theta,\theta_i)$ is the scattered far-field amplitude.

Boundary conditions on the contour Γ of the inhomogeneity are expressed in terms of the deflection $w(\mathbf{r})$, the normal slope $\gamma(\mathbf{r})$, the bending moment $M(\mathbf{r})$ and the generalized Kirchhoff stress $V(\mathbf{r})$:

$$M(\mathbf{r})=0,\quad V(\mathbf{r})=0,\quad \mathbf{r}\in\Gamma\quad \text{for absolutely soft inclusion,} \tag{4}$$

$$w(\mathbf{r})=0,\quad \gamma(\mathbf{r})=0,\quad \mathbf{r}\in\Gamma\quad \text{for absolutely hard inclusion.} \tag{5}$$

The fundamental solution of Eq. (1) is given by $G(\mathbf{r},\mathbf{r}_0)$. It is the solution of Eq. (1) with a Dirac's delta distribution as the load applied at the point $\mathbf{r}_0$:

$$(\Delta^2-k^4)G(\mathbf{r},\mathbf{r}_0)=\delta(\mathbf{r}-\mathbf{r}_0)/D. \tag{6}$$

It represents the transversal deflection of an infinitely extended plate at point $\mathbf{r}$ due to a unit concentrated lateral load at point $\mathbf{r}_0$. The solution of (6) has the form [21]

$$G(\mathbf{r},\mathbf{r}_0)=\frac{1}{8\pi Dk^2}[i\pi H_0^{(1)}(k|\mathbf{r}-\mathbf{r}_0|)-2K_0(k|\mathbf{r}-\mathbf{r}_0|)]. \tag{7}$$

In Eq. (7) $H_0^{(1)}(x)$ is the zero order Hankel function of the first kind, $K_0(x)$ is the zero order modified Bessel function of the second kind.

With the aid of Green's identity [21] and the fundamental solution (7) and its derivatives, it is possible to write an integral relation for the displacement w at point $\mathbf{r}\in\mathbb{R}^2$:

$$\int_\Gamma [V^G(\mathbf{r},\mathbf{r}')w(\mathbf{r}')-M^G(\mathbf{r},\mathbf{r}')\gamma(\mathbf{r}')]d\Gamma(\mathbf{r}')-\int_\Gamma [V(\mathbf{r}')G(\mathbf{r},\mathbf{r}')-M(\mathbf{r}')\gamma^G(\mathbf{r},\mathbf{r}')]d\Gamma(\mathbf{r}')+w^{in}(\mathbf{r})=\begin{cases} w(\mathbf{r}), & \mathbf{r}\in S\\ 0, & \mathbf{r}\in\overline{S}\end{cases} \tag{8}$$

In Eq. (8) S is the region of median surface of the plate outside of the inclusion, $V^G(\mathbf{r},\mathbf{r}')$, $M^G(\mathbf{r},\mathbf{r}')$and $\gamma^G(\mathbf{r},\mathbf{r}')$ represent the elements (2) derived from the fundamental solution (7) and, finally, $\overline{S}$ is the interior domain of the inclusion $(S\cup\overline{S}=\mathbb{R}^2/\Gamma)$.

Just as in acoustic and elastic bulk wave scattering process, certain reciprocity relation is satisfied in flexural wave scattering and it is given by

$$f(\theta,\theta_i)=f(\pi+\theta_i,\pi+\theta). \tag{9}$$

To prove this relation the similar procedure as in [22] may be used.

3. Determination of the transition matrix

With the purpose of finding a numerical solution to the exterior problems (1) and (4), (5) at the wave zone of a scatterer, we use the T-matrix approach [19]. Applying Graf's addition theorems to the special functions in the fundamental solution (7), we obtain

$$G(\mathbf{r},\mathbf{r}')=\frac{1}{8\pi Dk^2}\sum_{\sigma=1}^{2}\sum_{n=0}^{\infty}\varepsilon_n[i\pi\overline{\Phi}_{1\sigma n}(\mathbf{r}')\Phi_{1\sigma n}(\mathbf{r})-2\overline{\Phi}_{2\sigma n}(\mathbf{r}')\Phi_{2\sigma n}(\mathbf{r})],\quad |\mathbf{r}'|<|\mathbf{r}|,$$

$$\Phi_{\tau\sigma n}(\mathbf{r})=\Phi_{\tau n}(r)C_{\sigma n}(\theta),\quad \overline{\Phi}_{\tau\sigma n}(\mathbf{r})=\overline{\Phi}_{\tau n}(r)C_{\sigma n}(\theta),$$

$$\Phi_{\tau n}(r)=\begin{cases} H_n^{(1)}(kr), & \tau=1\\ K_n(kr), & \tau=2\end{cases},\quad \overline{\Phi}_{\tau n}(r)=\begin{cases} J_n^{(1)}(kr), & \tau=1,\\ I_n(kr), & \tau=2.\end{cases}$$

$$C_{\sigma n}(r)=\begin{cases}\cos n\theta, & \sigma=1\\ \sin n\theta, & \sigma=2\end{cases}\quad n=\overline{0,\infty}, \tag{10}$$

where ε_n is the Neumann factor, $J_n(x)$ are Bessel functions and $H_n^{(1)}(x)$ are Hankel functions of the first kind, $I_n(x)$ and $K_n(x)$ are the modified Bessel functions of the first and second kind, respectively.

The set $\{\Phi_{\tau\sigma n}(\mathbf{r})\}$ is a complete set suitable to represent the scattered waves everywhere outside the circle circumscribing the domain $\overline{S}$ and it corresponds to outgoing and exponentially decaying waves at infinity. To represent the incident field (with sources outside of the obstacle) we used the set $\{\overline{\Phi}_{\tau\sigma n}(\mathbf{r})\}$, regular at the origin. Thus we expand

$$w^{in}(r,\theta)=A_0\sum_{\tau=1}^{2}\sum_{\sigma=1}^{2}\sum_{m=0}^{\infty}a_{\tau\sigma m}\overline{\Phi}_{\tau\sigma m}(r,\theta),\quad r<\min_{\mathbf{r}\in\Gamma}|\mathbf{r}|,$$

$$w^{sc}(r,\theta)=A_0\sum_{\tau=1}^{2}\sum_{\sigma=1}^{2}\sum_{m=0}^{\infty}\alpha_{\tau\sigma m}\Phi_{\tau\sigma m}(r,\theta),\quad r>\max_{\mathbf{r}\in\Gamma}|\mathbf{r}|, \tag{11}$$

where $\alpha_{\tau\sigma m}$ are unknown coefficients to be determined, and $a_{1\sigma m}=\sqrt{\varepsilon_m}i^m C_{\sigma m}(\theta_i)$, $a_{2\sigma m}=0$. Putting expansions for w^{in}, w^{sc} and $G(\mathbf{r},\mathbf{r}')$ into Eq. (8), we get

$$\alpha_{\tau\sigma m}=\beta_\tau\int_\Gamma(\overline{V}_{\tau\sigma m}w(\mathbf{r}')-\overline{M}_{\tau\sigma m}\gamma(\mathbf{r}'))d\Gamma(\mathbf{r}'), \tag{12}$$

$$a_{\tau\sigma m}=\beta_\tau\int_\Gamma(V_{\tau\sigma m}w(\mathbf{r}')-M_{\tau\sigma m}\gamma(\mathbf{r}'))d\Gamma(\mathbf{r}'), \tag{13}$$

for a soft inhomogeneity and

$$\alpha_{\tau\sigma m}=\beta_\tau\int_\Gamma(\overline{\gamma}_{\tau\sigma m}M(\mathbf{r}')-\overline{\Phi}_{\tau\sigma m}V(\mathbf{r}'))d\Gamma(\mathbf{r}'), \tag{14}$$

$$a_{\tau\sigma m}=\beta_\tau\int_\Gamma(\gamma_{\tau\sigma m}M(\mathbf{r}')-\Phi_{\tau\sigma m}V(\mathbf{r}'))d\Gamma(\mathbf{r}'),\tag{15}$$

for a hard inhomogeneity. In Eq. (12)–(15) the bending moments $M_{\tau\sigma m}$ and $\overline{M}_{\tau\sigma m}$, the effective shear forces $V_{\tau\sigma m}$ and $\overline{V}_{\tau\sigma m}$, the normal slopes $\gamma_{\tau\sigma m}$ and $\overline{\gamma}_{\tau\sigma m}$ are defined by relations (2) if the function $w(r,\theta)$ is replaced by the functions $\Phi_{\tau\sigma m}(r,\theta)$ and $\overline{\Phi}_{\tau\sigma m}(r,\theta)$ in them, respectively, $\beta_\tau=(i\pi\delta_{\tau 1}-2\delta_{\tau 2})/(8\pi Dk^2)$, where $\delta_{\tau i}$ is the Kronecker delta.

From now on, we represent $w(\mathbf{r})$, $\gamma(\mathbf{r})$, and $M(\mathbf{r})$, $V(\mathbf{r})$, $\mathbf{r}\in\Gamma$, using the polar coordinates, in the form of truncated series:

$$w(\mathbf{r})=A_0\sum_{\sigma=1}^{2}\sum_{n=0}^{M}x^s_{1\sigma n}C_{\sigma n}(\theta),\quad \gamma(\mathbf{r})=A_0a^{-1}\sum_{\sigma=1}^{2}\sum_{n=0}^{M}x^s_{2\sigma n}C_{\sigma n}(\theta),\quad \mathbf{r}\in\Gamma,$$

$$M(\mathbf{r})=A_0Da^{-2}\sum_{\sigma=1}^{2}\sum_{n=0}^{M}x^h_{1\sigma n}C_{\sigma n}(\theta),\quad V(\mathbf{r})=A_0Da^{-3}\sum_{\sigma=1}^{2}\sum_{n=0}^{M}x^h_{2\sigma n}C_{\sigma n}(\theta),\quad \mathbf{r}\in\Gamma,\tag{16}$$

where a is the characteristic dimension of the inhomogeneity, $M\to\infty$.

Substituting this expansions into Eqs. (13) and (15) we obtain an infinite system of linear algebraic equations for unknown coefficients $x^l_{\tau\sigma n}$, $l=s$, h. In the matrix notation we have

$$\begin{pmatrix}\mathbf{Q}^l_{1,1} & \mathbf{Q}^l_{1,2}\\ \mathbf{Q}^l_{2,1} & \mathbf{Q}^l_{2,2}\end{pmatrix}\begin{pmatrix}x^l_1\\ x^l_2\end{pmatrix}=\begin{pmatrix}\mathbf{a}_1\\ \mathbf{a}_2\end{pmatrix}.\tag{17}$$

Similarly, from Eqs. (12) and (14), we obtain

$$\begin{pmatrix}\overline{\mathbf{Q}}^l_{1,1} & \overline{\mathbf{Q}}^l_{1,2}\\ \overline{\mathbf{Q}}^l_{2,1} & \overline{\mathbf{Q}}^l_{2,2}\end{pmatrix}\begin{pmatrix}\mathbf{x}^l_1\\ \mathbf{x}^l_2\end{pmatrix}=\begin{pmatrix}\boldsymbol{\alpha}_1\\ \boldsymbol{\alpha}_2\end{pmatrix},\tag{18}$$

where $\mathbf{x}^l_\tau$, $\mathbf{a}_\tau$, $\boldsymbol{\alpha}_\tau$ denotes column matrices formed by $x^l_{\tau\sigma n}$, $a_{\tau\sigma m}$, $\alpha_{\tau\sigma m}$, respectively. The elements of the matrices $\mathbf{Q}^l_{\tau,\tau'}$ are

$$Q^s_{\tau\sigma m,1\sigma' n}=-\beta_\tau\int_\Gamma V_{\tau\sigma m}(r,\theta)C_{\sigma' n}(\theta)\,\mathrm{d}\Gamma,\quad Q^s_{\tau\sigma m,2\sigma' n}=\beta_\tau a^{-1}\int_\Gamma M_{\tau\sigma m}(r,\theta)C_{\sigma' n}(\theta)\,\mathrm{d}\Gamma,$$

$$Q^h_{\tau\sigma m,1\sigma' n}=-\beta_\tau Da^{-2}\int_\Gamma\gamma_{\tau\sigma m}(r,\theta)C_{\sigma' n}(\theta)\,\mathrm{d}\Gamma,$$

$$Q^h_{\tau\sigma m,2\sigma' n}=\beta_\tau Da^{-3}\int_\Gamma\Phi_{\tau\sigma m}(r,\theta)C_{\sigma' n}(\theta)\,\mathrm{d}\Gamma.\tag{19}$$

The expressions for $\overline{Q}^l_{\tau\sigma m,\tau'\sigma' n}$ contain functions $\overline{V}_{\tau\sigma m}$, $\overline{M}_{\tau\sigma m}$, $\overline{\gamma}_{\tau\sigma m}$ and $\overline{\Phi}_{\tau\sigma m}$ instead of functions $V_{\tau\sigma m}$, $M_{\tau\sigma m}$, $\gamma_{\tau\sigma m}$ and $\Phi_{\tau\sigma m}$ in integrands of Eqs. (19), respectively.

Solving formally the matrix Eqs. (17) and (18), we obtain the transition matrix $\mathbf{T}$, that relate coefficients $a_{\tau\sigma m}$ with coefficients $\alpha_{\tau\sigma m}$:

$$\begin{pmatrix}\boldsymbol{\alpha}_1\\ \boldsymbol{\alpha}_2\end{pmatrix}=\begin{pmatrix}\mathbf{T}_{1,1} & \mathbf{T}_{1,2}\\ \mathbf{T}_{2,1} & \mathbf{T}_{2,2}\end{pmatrix}\begin{pmatrix}\mathbf{a}_1\\ \mathbf{a}_2\end{pmatrix},$$

$$\mathbf{T}=\begin{pmatrix}\mathbf{T}_{1,1} & \mathbf{T}_{1,2}\\ \mathbf{T}_{2,1} & \mathbf{T}_{2,2}\end{pmatrix}=\begin{pmatrix}\overline{\mathbf{Q}}^l_{1,1} & \overline{\mathbf{Q}}^l_{1,2}\\ \overline{\mathbf{Q}}^l_{2,1} & \overline{\mathbf{Q}}^l_{2,2}\end{pmatrix}\begin{pmatrix}\mathbf{Q}^l_{1,1} & \mathbf{Q}^l_{1,2}\\ \mathbf{Q}^l_{2,1} & \mathbf{Q}^l_{2,2}\end{pmatrix}^{-1},\tag{20}$$

or

$$\mathbf{T}=\overline{\mathbf{Q}}^l(\mathbf{Q}^l)^{-1}.\tag{21}$$

The $\mathbf{T}$ matrix depends only on the nature and shape of the obstacle and does not depend on the incident field. The requirements of reciprocity and energy conservation impose additional constraints on the transition matrix. To derive these constraints, notice that the far-field amplitude may be obtained from Eq. (11) and can be written as

$$f(\theta,\theta_i)=\sum_{\sigma=1}^{2}\sum_{m=0}^{\infty}a^*_{1\sigma m}(\theta)\alpha_{1\sigma m}(\theta_i),\tag{22}$$

or in the matrix notation

$$f(\theta,\theta_i)=a^{*t}(\theta)\mathbf{T}_{1,1}a(\theta_i)=\mathbf{b}^{*t}(\theta)\mathbf{T}\mathbf{b}(\theta_i),\quad \mathbf{b}(\theta)=\begin{pmatrix}\mathbf{a}(\theta)\\ \mathbf{0}\end{pmatrix},\tag{23}$$

where $\mathbf{a}(\theta)$ denotes the column matrix formed by $a_{1\sigma m}(\theta)$, the asterisk indicates a complex conjugate and a superscript t indicates transpose of the matrix. Since $a_{1\sigma m}(\pi+\theta)=a_{1\sigma m*}(\theta)$, we obtain

$$f(\pi+\theta_i,\pi+\theta)=\mathbf{b}^{*t}(\theta)\mathbf{T}^t\mathbf{b}(\theta_i). \tag{24}$$

The reciprocity relation, Eq. (9) then implies that $\mathbf{T}$ matrix is symmetric

$$\mathbf{T}=\mathbf{T}^t. \tag{25}$$

The expression of energy conservation is related to the optic theorem [6]

$$\sigma^{sc}=\frac{2}{\pi k}\int_0^{2\pi}|f(\theta,\theta_i)|^2\,\mathrm{d}\theta=-\frac{4}{k}\,\mathrm{Re}\,f(\theta_i,\theta_i), \tag{26}$$

where $\sigma^{sc}$is the scattering cross-section. Substituting Eq. (23) into Eq. (26), we obtain

$$\mathbf{a}^t(\theta_i)(\mathbf{T}^t_{1,1})(\mathbf{T}^*_{1,1})\mathbf{a}^*\ (\theta_i)=-\mathbf{a}^t(\theta_i)\mathrm{Re}(\mathbf{T}_{1,1})\mathbf{a}^*\ (\theta_i) \tag{27}$$

and thus

$$\mathbf{T}_{1,1}\mathbf{T}^*_{1,1}=-\mathrm{Re}\,\mathbf{T}_{1,1}. \tag{28}$$

The properties (25) and (28) of the $\mathbf{T}$ matrix are particularly important since they are indispensable for checking the accuracy of the numerical calculations.

It is well known that the scattering cross-section for a single obstacle is proportional to the wave attenuation coefficient β in the medium containing dilute concentration and stochastically distributed the equal obstacles [6]

$$\beta=(n/2)\sigma^{sc}=-\frac{2c}{ks_0}\mathbf{a}^t(\theta_i)\mathrm{Re}(\mathbf{T}_{1,1})\mathbf{a}^*\ (\theta_i), \tag{29}$$

where s_0 is the area of a single obstacle, c is the inclusion density parameter (the quantity $n=c/s_0$ corresponds to the number density of the inclusions). For the case of randomly oriented obstacle, the average of Eq. (29) over the angle

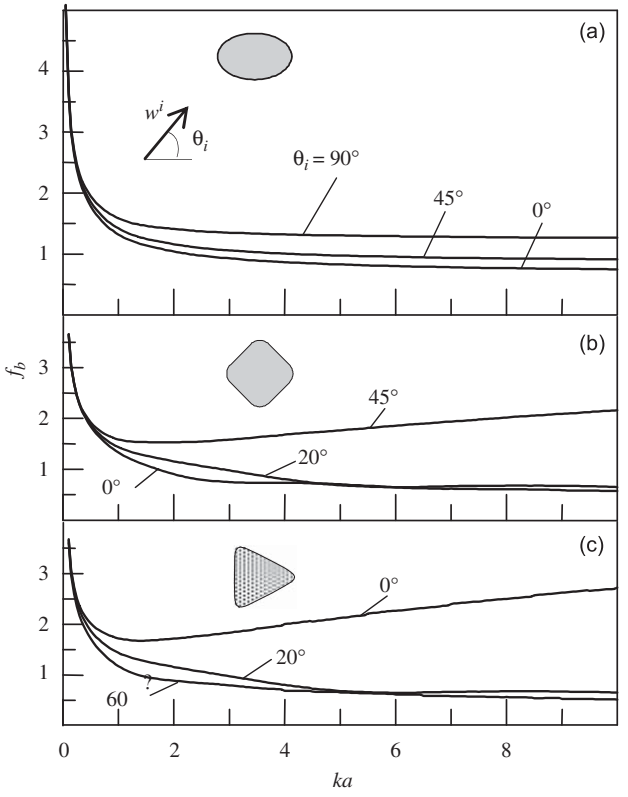

Fig. 1. The magnitude of the backscattered far-field amplitude in plate with rigid inclusion of (a) elliptic form ($N=1,\varepsilon=0.2$), in Eq. (31)), (b) square form ($N=3,\varepsilon=1/9$) and (c) triangle form ($N=2,\varepsilon=0.25$).

θ_i must provide

$$\beta = \frac{n}{4\pi}\int_0^{2\pi} \sigma^{sc}(\theta_i)\,\mathrm{d}\theta_i = -\frac{2c}{ks_0}\sum_{\sigma=1}^{2}\sum_{m=0}^{\infty} \mathrm{Re}\,T_{1\sigma m,1\sigma m} \tag{30}$$

Consequently, the expressions (21), (23), (29) and (30) give the solution of the problem in the far wave zone of a scatterer.

4. Numerical examples

As an example let us consider a case when the inclusion shape is given by the parametric equation

$$r(\varphi) = a\sqrt{\frac{1+\varepsilon^2+2\varepsilon\cos(N+1)\varphi}{1-\varepsilon^2 N}},\quad \theta(\varphi) = \mathrm{arctg}\frac{\sin\varphi-\varepsilon\sin N\varphi}{\cos\varphi+\varepsilon\cos N\varphi},\quad 0\le\varphi\le 2\pi, \tag{31}$$

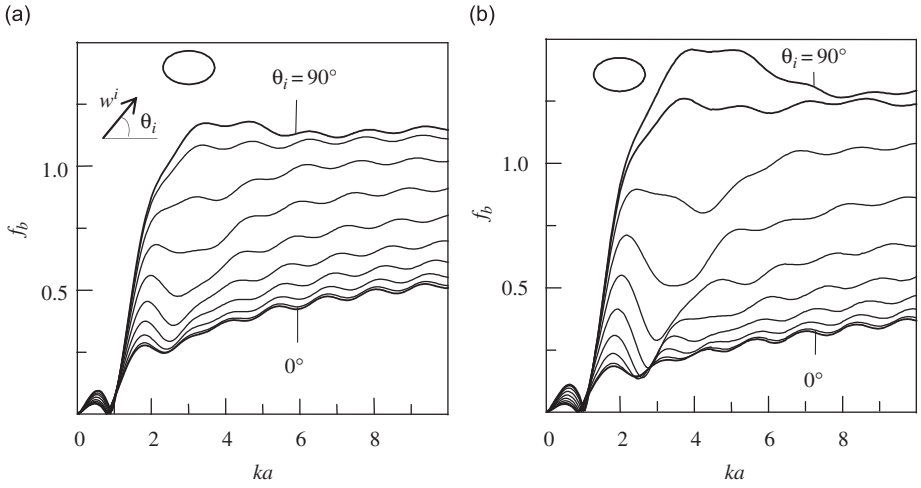

Fig. 2. Backscattered amplitude from elliptic hole ((a) $\varepsilon = 0.2$, (b) $\varepsilon = 0.3$) for incident angles from 0° to 90° in steps of 10°.

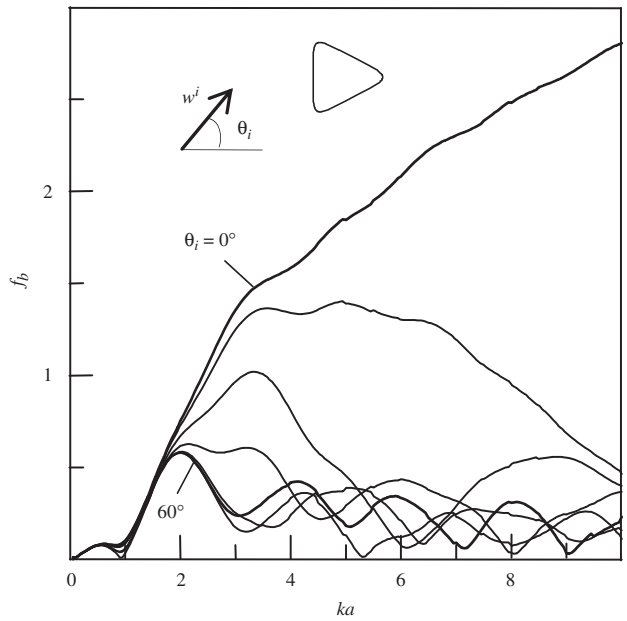

Fig. 3. Backscattered amplitude from triangle hole ($N = 2, \varepsilon = 0.25$) for incident angles from 0° to 60° in steps of 10°.

where $0 \le \varepsilon < 1$, N is a natural number. For particular values N and variables ε we obtain some set of contours. In particular, for $N=1$ we have ellipses with aspect ratio $(1-\varepsilon)/(1+\varepsilon)$, for $N=2$—triangles, for $N=3$—squares with rounded corners. The area of obstacle is $s_0 = \pi a^2$.

It is obvious that in numerical calculations the parameter Min expansion (16) is limited and unknown quantities can be calculate with sufficient accuracy by approximate numerical procedures. Indeed, an accuracy of one percent is obtained if $M=12$ for $ka \le 3$, $M = 2ka+6$ (truncated to closest integer) for $3 < ka \le 10$.

Figs. 1–4 present the modulus of backscattering amplitude $f_b = |f(\pi+\theta_i, \theta_i)|$ versus dimensionless wavenumber ka for various angles of incidences θ_i and form of inclusions. Calculations have been performed for a steel plate with Poisson's ratio 0.26. The response from the rigid inclusions (Fig. 1) increases without bound as the frequency tends to zero

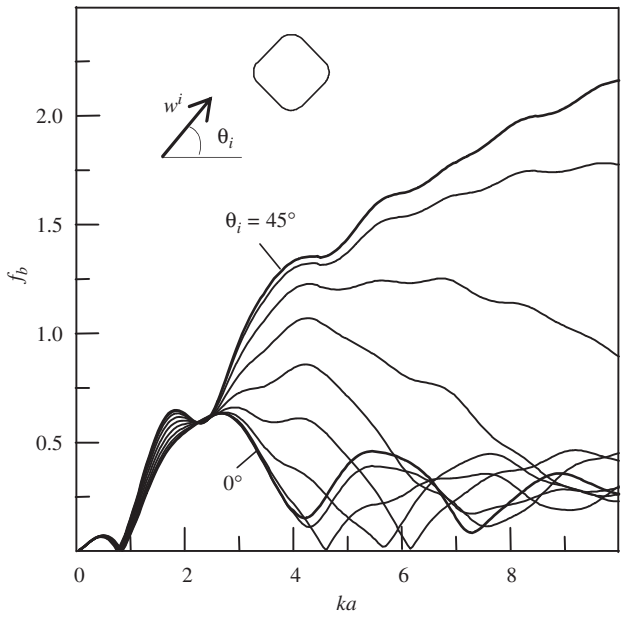

Fig. 4. Backscattered amplitude from square hole ($N=3, \varepsilon = 1/9$) for incident angles from 0° to 45° in steps of 5°.

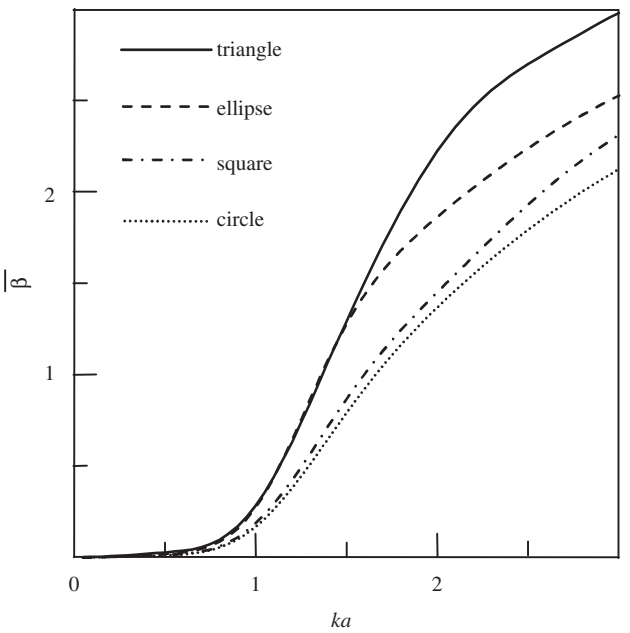

Fig. 5. Effect of hole forms on attenuation of flexural wave in steel plate with randomly distributed and randomly oriented holes.

(the static limit). This is to be expected, and has been discussed by Norris and Vemula [6] for scattering of flexural wave from a circular rigid inclusion.

The backscattering amplitudes for a hole (Figs. 2–4) oscillate with increasingka. This oscillation is due to interference of the wave specularly reflected from the front hole and waves diffracted on the hole. In frequency range $ka>2$ the largest for f_b values correspond to normal wave incidence on the quasi flat part of the hole ($\theta_i=90^\circ$ for ellipses, $\theta_i=0^\circ$ for triangle and $\theta_i=45^\circ$ for square hole).

Note that numerical calculations of the backscattering amplitude for a rigid circular inclusion and a circular hole ($\varepsilon=0$ in Eq. (31)) are in complete accordance with corresponding data given by Norris and Vemula [6].

Fig. 5 presents the frequency dependences of normalized attenuation coefficients $\overline{\beta}=(2\pi\alpha/c)\beta$ in steel plates with randomly distributed and randomly oriented holes of circular ($\varepsilon=0$), elliptic ($N=1,\varepsilon=0.3$), square ($N=3,\varepsilon=1/9$) and triangle ($N=2,\varepsilon=0.25$) shapes. The hole of different forms has the same area. As it is seen, for all forms of holes we observe the increase of parameter $\overline{\beta}$ when the frequency increases. Attenuation of the flexural wave in the plate with randomly distributed holes of triangular form reaches the higher value than other forms of the hole.

5. Conclusions

It has been shown that the T-matrix method can be used to investigate the flexural wave scattering in a two-dimensional thin plate with a through inhomogeneity of complex geometry. In particular, when the exact analytical solution cannot be obtained, the improved T-matrix is direct and elegant. The scattering matrix, that related the outgoing waves with ingoing, is $\mathbf{S}=\mathbf{1}+2\mathbf{T}_{1,1}$. From properties (25) and (28) we see that S matrix is symmetric and unitary.

We have presented the scattering problem for a limited case of scatterer: hole and rigid inclusion. One advantage of the present method is that it can be easily adopted to scattering of flexural wave by inclusions with arbitrary plate properties and can be extended to analyse the vibration control of plate-like structures. Numerical examples show that the proposed approach has great advantage in programming easily, higher efficiency and accuracy, and is reliable compared with the wave function expansion method.

References

[1] P. Fromme, P. Wilcox, M.J.S. Lowe, P. Cawley, On the development and testing of a guided ultrasonic wave array for structural integrity monitoring, *IEEE Transactions on Ultrasonics, Ferroelectrics, and Frequency Control* 53 (2006) 777–785.
[2] J.D. Achenbach, *Wave Propagation in Elastic Solids*, North-Holland, Amsterdam, 1973.
[3] B. Auld, *Field and Waves in Solids*, Krieger, Malabar, Florida, 1990.
[4] Y.H. Pao, C.C. Chao, Diffractions of flexural waves by a cavity in an elastic plate, *AIAA Journal* 2 (1964) 2004–2010.
[5] T.-H. Lu, Diffraction of Flexural Waves by a Circular Rigid Inclusion in an Elastic Plate and Dynamic Stress Concentration, Master's Thesis, National Taiwan University, Taiwan, 1966.
[6] A.N. Norris, C. Vemula, Scattering of flexural waves on thin plates, *Journal of Sound and Vibration* 181 (1995) 115–125.
[7] C. Vemula, A.N. Norris, Flexural wave propagation and scattering on thin plates using Mindlin theory, *Wave Motion* 26 (1997) 1–12.
[8] Yu.I. Bobrovnitskii, On the energy flow in evanescent waves, *Journal of Sound and Vibration* 152 (1992) 175–176.
[9] R.H. Lande, R.S. Langley, The energetics of cylindrical bending waves in a thin plate, *Journal of Sound and Vibration* 279 (2005) 513–518.
[10] J.C.P. McKeon, M.K. Hinders, Lamb waves scattering from a through hole, *Journal of Sound and Vibration* 224 (1999) 843–862.
[11] P. Fromme, M.B. Sayir, Measurement of the scattering of a Lamb wave by a through hole in a plate, *Journal of the Acoustical Society of America* 111 (2002) 1165–1170.
[12] R. Paskaramoorthy, A.H. Shah, S.K. Datta, Scattering of flexural waves by cavities in a plate, *International Journal of Solids and Structures* 25 (1989) 1177–1191.
[13] O. Diligent, T. Grahn, A. Boström, P. Cawley, M.J.S. Lowe, The low-frequency reflection and scattering of the S_0 Lamb mode from a circular through-thickness hole in a plate: Finite element analytical and experimental studies, *Journal of the Acoustical Society of America* 112 (2002) 2589–2601.
[14] O. Diligent, M.J.S. Lowe, Reflection of the S0 Lamb mode from a flat bottom circular hole, *Journal of the Acoustical Society of America* 118 (2005) 2869–2879.
[15] S.Z. Peng, Flexural wave scattering and dynamic stress concentration in a heterogeneous plate with multiple cylindrical patches by acoustical wave propagator techniques, *Journal of Sound and Vibration* 286 (2005) 729–743.
[16] C.H. Wang, F. Chang, Scattering of plate waves by a cylindrical inhomogeneity, *Journal of Sound and Vibration* 282 (2005) 429–451.
[17] T. Grahn, Lamb wave scattering from a circular partly through-thickness hole in a plate, *Wave Motion* 37 (2003) 63–80.
[18] F.B. Cegla, A. Rohde, M. Veidt, Analytical prediction and experimental measurement for mode conversion and scattering of plate waves at non-symmetric circular blind holes in isotropic plates, *Wave Motion* 45 (2008) 162–177.
[19] P.C. Waterman, Matrix theory of elastic wave scattering, *Journal of the Acoustical Society of America* 60 (1976) 567–580.
[20] P.A. Martin, On connections between boundary integral equations and T-matrix methods, *Engineering Analysis with Boundary Elements* 27 (2003) 771–777.
[21] M. Kitahara, *Boundary Integral Equation Methods in Eigenvalue Problems of Elastodynamics and Thin Plates*, Elsevier, Amsterdam, 1985.
[22] R. Kress, Scattering by obstacles, in: R. Pike, P. Sabatier (Eds.), *Scattering: Scattering and Inverse Scattering in Pure and Applied Science*, Academic Press, London, 2002, pp. 52–73.